

Primordial atmosphere incorporation in planetary embryos and the origin of Neon in terrestrial planets



Etienne Jaupart^{a,*}, Sébastien Charnoz^b, Manuel Moreira^b

^aEcole Normale Supérieure de Lyon, Lyon Cedex 07, France

^bInstitut de Physique du Globe de Paris, Sorbonne Paris Cité, UMR CNRS 7154, Université Paris Diderot, France

ARTICLE INFO

Article history:

Received 12 April 2016

Revised 1 February 2017

Accepted 18 April 2017

Available online 27 April 2017

Keywords:

Primordial atmospheres

Atmospheric structures

Thermodynamic equilibrium

Origin of Neon in terrestrial planets

ABSTRACT

The presence of Neon in terrestrial planet mantles may be attributed to the implantation of solar wind in planetary precursors or to the dissolution of primordial solar gases captured from the accretionary disk into an early magma ocean. This is suggested by the Neon isotopic ratio similar to those of the Sun observed in the Earth mantle. Here, we evaluate the second hypothesis. We use general considerations of planetary accretion and atmospheric science. Using current models of terrestrial planet formation, we study the evolution of standard planetary embryos with masses in a range of 0.1–0.2 M_{Earth} , where M_{Earth} is the Earth's mass, in an annular region at distances between 0.5 and 1.5 Astronomical Units from the star. We determine the characteristics of atmospheres that can be captured by such embryos for a wide range of parameters and calculate the maximum amount of Neon that can be dissolved in the planet. Our calculations may be directly transposed to any other planet. However, we only know of the amount of Neon in the Earth's solid mantle. Thus we use Earth to discuss our results. We find that the amount of dissolved Neon is too small to account for the present-day Neon contents of the Earth's mantle, if the nebular gas disk completely disappears before the largest planetary embryos grow to be $\sim 0.2 M_{\text{Earth}}$. This leaves solar irradiation as the most likely source of Neon in terrestrial planets for the most standard case of planetary formation models.

© 2017 Elsevier Inc. All rights reserved.

1. Introduction

The atmospheres of Mars, Venus and Earth have evolved through time and bear the signature of late processes such as the post-accretion addition of a volatile-rich veneer and/or mantle degassing. ^3He emissions at mid ocean ridges demonstrate that the Earth's mantle is still losing primordial gases today, e.g. [Clarke et al. \(1969\)](#) and [Craig et al. \(1975\)](#), indicating long-term storage in the deep mantle. Gaseous species that are found in the Earth's mantle have probably been inherited from solar gases captured during planetary formation (e.g. [Sasaki, 1999](#)). This is particularly true for Neon, the second noble gas and the fifth element in the solar system by order of abundance, because its $^{20}\text{Ne}/^{22}\text{Ne}$ isotopic ratio is "solar-like" ([Sarda et al., 1988](#); [Honda et al., 1991](#)). Relative to the isotopic composition of the atmosphere, the $^{20}\text{Ne}/^{22}\text{Ne}$ ratio in the source of oceanic basalts takes values that are larger than 12.5 and that can be as high as 12.8, close to the solar value of ~ 13.8 ([Mukhopadhyay, 2012](#); [Yokochi](#)

and [Marty, 2004](#); [Kurz et al., 2009](#); [Colin et al., 2015](#); [Moreira and Charnoz, 2016](#)). Two processes have been invoked for account for the presence of solar-like Neon in the Earth's mantle. Solar gases were present in the atmospheres of planetary embryos and got dissolved in an early magma ocean ([Sasaki, 1999](#)). Alternatively, solar gases may have been carried by solar wind and got implanted in planetary precursors ([Tieloff, 2000](#); [Raquin and Moreira, 2009](#); [Moreira and Charnoz, 2016](#)).

According to our current understanding of terrestrial planetary formation, the Earth likely grew from a swarm of planetary embryos shortly after the formation of the oldest known solids within of the solar system, Calcium Aluminium Rich inclusions (CAIs) found in meteorites with an age of 4.567 Gy ([Amelin et al., 2002](#)). According to ^{182}Hf – ^{182}W studies of mantle-derived samples, the Earth's core was last equilibrated within the first 50 Myrs ([Kleine et al., 2009](#)). The planetary embryos that coalesced into Earth, however, were formed much earlier, only 1–2 millions years after the CAIs. There are two competing theories of embryo formation.

The standard model of planetary embryo formation involves a swarm of planetesimals (~ 10 km objects at 1 AU from the Sun) e.g. [Greenberg et al. \(1984\)](#). These planetesimals go through a phase of

* Corresponding author.

E-mail address: etienne.jaupart@ens-lyon.fr (E. Jaupart).

"runaway growth" with low velocity impacts that lasts less than 1 Myr. Numerical simulations show that the largest objects grow at much larger rates than their smaller neighbors, leading to the rapid formation of a locally dominant body. Due to rapid material depletion in its surroundings and to the progressive dynamical excitation of neighboring planetesimals, however, accretion stops when the largest local body reaches the so-called "Isolation Mass" (Lissauer, 1987). Such bodies have masses between those of Moon and Mars, depending on the local disk surface density and distance to the Sun. In the absence of external perturbations, locally dominant bodies are separated from their neighbors by about 10 mutual Hill radii, as in the "Grand Tack" model, see Walsh et al. (2011). In such conditions, they are dynamically isolated and it takes another ~ 100 Myrs for them to collide with one another and form Earth-sized planets. Thus, even though Earth may have accreted in 100 Myrs, its embryos may have already existed one million years or less after the formation of CAIs.

Recently, an alternative process of embryo formation has emerged, the so-called "Streaming Instability" model of Johansen and Klahr (2011). According to this model, embryos may have grown directly out of pebble-sized objects through an efficient accretion process enhanced by aerodynamic drag. In the Solar Nebula, dust coagulation leads rapidly to millimeter-sized objects at 1 AU distance (Brauer et al., 2008) and even larger objects if it occurs in a turbulent free region (Charnoz and Taillifet, 2011). These objects are marginally coupled to the ambient gas and settle rapidly to the mid-plane of the disk, expelling gas from the mid-plane. High-pressure regions collect pebbles with increasing efficacy through the so-called "streaming instability" process, leading to the growth of large bodies that eventually collapse gravitationally in a few orbits (Johansen et al., 2007). The maximum size of such bodies is not well constrained, but it seems possible that they reach sizes of at least of a few hundred kilometers or larger. In that case, "planetesimals" would not even exist and embryos may form directly in a very short time because of the coupled effects of accretion and aerodynamic drag. This process may account for the small mass of Mars (Levison et al., 2015) and may also explain the large initial dimensions of asteroids (Morbidelli et al., 2009).

Protoplanet formation takes a few millions years only and is accompanied by the gradual disappearance of the gas disk progressively due to photo-evaporation (Hillenbrand, 2005). A few million years later, the gas disk has completely evaporated (Gorti et al., 2009), leaving a population of planetary embryos that accrete to form planets.

According to the above sequence and timing of events, planetary embryos were kept immersed in a gaseous protoplanetary disk for a couple of million years, well before they could assemble into a fully grown planet. During this phase, while their mass was between 0.1 to 10% of that of Earth, they may have captured a primitive atmosphere composed of gas from the protosolar nebula with a solar composition. In this study, we determine the structure of such a proto-atmosphere. The mantle of the planetary embryos, if it was molten, equilibrated with the captured atmosphere, leading to the dissolution of noble gases in potentially significant quantities.

This problem has been addressed in the past literature, but the conclusions given were different. Sasaki and Nakazawa (1990) for example treated this issue for embryos with a range of mass from 0.5 to 1 M_{Earth} in a still present and massive disk. Using the geochemical constraints available at that time on Neon dissolution they concluded that the solar type atmosphere around the protoplanet should have started escaping before the planetary mass was lower than 0.6 M_{Earth} . In this paper we used updated models of planetary formation and updated geochemical constraints, which lead us to study embryos with mass of 0.1 and 0.2 M_{Earth} and compare the efficiency of the atmospheric dissolution process against

estimations of the Neon concentration before the degassing of the mantle. Standard cases of recent models of planetary formation only produce Earth embryos as small as 0.1 to 0.2 Earth mass for the biggest objects when the gaseous disk is still massive and present (e.g. Walsh and Levison, 2016). We thus study a standard embryo of 0.1 to 0.2 M_{Earth} and use updated geochemical constraints which allows us to give different conclusions that the ones drawn in the previous literature.

2. Numerical method

2.1. Model

We assume that the atmosphere is spherically-symmetric and segues into the surrounding nebula at its outer radius r_{atm} , which will be defined below. For simplicity, we assume that the planet is much heavier than its atmosphere, which is appropriate for this study, implying that the atmosphere does not modify the gravity field due to the planet. The atmospheric structure is well described by the equation of hydrostatic equilibrium.

$$\frac{dP}{dr} = -\frac{GM_{core}\rho}{r^2} \quad (1)$$

where P and ρ are respectively the pressure and density of atmospheric gas, r the distance to the planet center, G the gravitational constant and M_{core} the planet mass.

The thermal structure can be obtained from the energy balance equation. The optical thickness is denoted by τ :

$$\tau \equiv \int_r^{r_{atm}} \kappa \rho dr \quad (2)$$

If τ is smaller than 2/3 and provided that the radial temperature gradient is less than the adiabatic one, temperature obeys the following equation (Hayashi et al., 1979) :

$$T^4 = T_{disk}^4 + \frac{L}{8\pi\sigma r^2} \frac{1 + 3\tau/2}{2 - 3\tau/2} \quad (3)$$

In Eqs. (2) and (3), T and T_{disk} are the temperature of the atmosphere at radius r and the temperature in the disk, respectively, and κ is the Rosseland opacity.

If $\tau > 2/3$, the radial temperature distribution is given by the lesser of the adiabatic and radiative temperature gradients. Considering the ideal gas equation of state, the former is given by:

$$\frac{dT_{ad}}{dr} = -\frac{\gamma - 1}{\gamma} \frac{GM_{core}\mu}{k_B r^2} \quad (4)$$

whereas the latter is given by:

$$\frac{dT_{rad}}{dr} = -\frac{3\kappa\rho L}{64\pi\sigma r^2 T^3} \quad (5)$$

where $\gamma = C_p/C_v$ is the adiabatic exponent and is equal to 7/5 in this study, k_B is the Boltzmann constant and μ the mass of a single molecule of gas taken to be 2.34 m_{proton} . L is the energy flux passing through a sphere of radius r and is called luminosity. Rosseland opacities are taken from Baillié et al. (2015) (see below). If the radiative gradient is larger than the adiabatic one, the atmosphere is unstable to convection, implying that the radial temperature profile adjusts to that of a well-mixed convective layer, which is well described by the adiabatic gradient.

If the embryo surface is partially molten ($T > \approx 1500$ K), we may use Henry's law to calculate the concentration of dissolved Neon that is in equilibrium with the atmospheric value:

$$c = s P_i \quad (6)$$

where c is the concentration of the dissolved gas, s solubility and P_i the partial pressure of the gas. In the following, we integrate Eqs. (1) to (5) using a fourth order Runge-Kutta method for a wide parameter range.

2.2. Inputs

The ranges of temperatures and density considered here are too low ($\log(T) < 3.5$) to allow the dissociation of hydrogen molecules (Saumon et al., 1995), and we consider a gas of solar composition (with the same composition as that of the disk) with molecular hydrogen. We use an ideal equation of state for this gas.

Opacities are taken from Baillié et al. (2015) and account for temperature-dependent physical properties of material composing the disk. For $T < 1500$ K, silicate material composing the dust is assumed to sublimate, implying that grain opacity is the largest contributor to the total opacity. The distribution of dust grains in the atmosphere is highly uncertain, however, so that we add a depletion factor f such that until 1500 K, $\kappa \simeq f \kappa_{\text{Baillié}}$, for $0 < f < 1$.

We limit ourselves to Earth formation scenarios and hence focus on protoplanets with masses in a 0.1 to 0.2 M_{Earth} range in 1 M year old nebula at distances between 0.5 and 1.5 AU from the star. At that time, embryos have been formed but the gas is still present in the disk.

To describe our 1 M year old nebula, we use MMSN profiles from Weidenschilling (1977) and Hayashi (1981):

Surface density profile

$$\Sigma(r) = 17000 \left(\frac{r}{1\text{AU}}\right)^{-1.5} \text{ kg/m}^2 \quad (7)$$

Temperature profile

$$T(r) = 500 \left(\frac{r}{1\text{AU}}\right)^{-0.5} \text{ K} \quad (8)$$

This density profile comes from a static version of the MMSN. In reality, the nebula evolves and its density decreases with time (Baillié et al., 2015). Maintaining a massive nebula (between 0.5 and 1.5 AU) leads to an upper bound for the equilibrium Neon concentration in embryos.

The solubility of Neon in basaltic melt is $25 \cdot 10^{-5}$ cc/g bar, following (Jambon et al., 1986). This solubility law relies on the assumption of thermodynamic equilibrium between the molten mantle and the atmosphere and specifies the maximum amount that can be dissolved.

2.3. Boundary conditions

A protoplanet with mean density ρ_p (equal to $3.9 \times 10^3 \text{ kg/m}^3$ in this study) has radius $R_{\text{core}} = \left(\frac{3M_{\text{core}}}{4\pi\rho_p}\right)^{1/3}$. Its atmosphere extends from $r = R_{\text{core}}$ to the smaller of the Hill and Bondi radii R_H and R_B defined as follows:

$$R_H = \left(\frac{M_{\text{core}}}{3M_*}\right)^{1/3} a \quad (9)$$

and

$$R_B = \frac{2GM_{\text{core}}\mu}{k_B T_{\text{disk}}} \quad (10)$$

where M_* is the Sun mass and a the distance to the Sun's center. At the Hill radius, the planetary gravity is equal to the tidal force due to the Sun, such that beyond this radial distance a gas particle cannot be considered to be gravitationally bound to the protoplanet. At the Bondi radius, the disk thermodynamic speed is equal to the escape velocity, such that beyond this point a particle of gas can escape the proto-planet's gravitational attraction. From Mars-sized to Earth-sized bodies, the Bondi radius is the smaller than the Hill one, and hence we assume that $r_{\text{atm}} = R_B$.

At its outer edge (at $r = r_{\text{atm}} = R_B$), the atmosphere is assumed to segue smoothly into the disk so that:

$$T(r_{\text{atm}}) = T_{\text{disk}} \text{ and } P(r_{\text{atm}}) = P_{\text{disk}} \quad (11)$$

Conditions at the base of the atmosphere against the solid or molten protoplanet are more complicated. In the case of thick and radiative atmospheres, the atmosphere acts very much like a solid black body and there is no atmospheric boundary layer above the ground. One can thus extend the bulk atmosphere temperature gradient down to $r = R_{\text{core}}$. In the presence of convection, there is a thin boundary layer above the proto-planet surface, where temperature rises rapidly towards the bulk atmospheric profile. In this case, one must therefore allow for a temperature difference between the ground and the base of the bulk atmospheric profile.

2.4. Parameters

For a given disk structure, the parameters of our model are the protoplanet mass M_{core} , its distance to the Sun a , luminosity L and grain depletion factor f . Following recent Earth formation scenarios, we consider 0.1 and 0.2 M_{Earth} embryos at distances between 0.5 and 1.5 AU from the Sun. 0.1 M_{Earth} embryos are supposed to be more abundant than 0.2 M_{Earth} after about 1 M year after and until the gas disappears in this annular region (see Weidenschilling et al., 1997).

Values of luminosity L are not well-known. It is often assumed to be set by the incoming flux of planetesimals in the accretion stage, such that it may be written as follows:

$$L \simeq \frac{GM_{\text{core}}\dot{M}}{R_{\text{core}}} \quad (12)$$

where \dot{M} is the accretion rate. Using this equation leads to ground temperatures that are less than 1500 K (melting point of silicates) for Mars-sized bodies (with $M \sim 0.1 M_{\text{Earth}}$) (Ikoma and Genda, 2006). We seek an upper bound to the concentration of Neon that can be dissolved in the protoplanet and hence allow for a wide range of values of L .

The range of values for the grain depletion factor f is also uncertain. However, the most significant change due to the depletion factor comes from Eq. (5), which involves $\kappa L \simeq f \kappa_{\text{Baillié}} L$. Thus, calculations with different values of L and f , but with fL kept constant, are expected to lead to similar results, which is confirmed by Ikoma and Genda (2006). Because we allow for a wide range of L , we take $f = 1$ in the following.

3. Results

3.1. Properties of the atmosphere

Most of the dependence of atmospherical characteristics on luminosity was already presented by Ikoma and Genda (2006) in their study of a 0.1 M_{Earth} embryo's atmosphere and our results are similar to theirs. We redevelop here these results more lengthily, because they are needed to explain our approach to calculate the amount of Neon that can be dissolved in the mantle.

Results for bodies with masses in a range of 0.1 to 0.2 M_{Earth} exhibit the same dependence on luminosity. Their atmospheres are fully radiative at low values of luminosity and fully convective at high values of luminosity. For intermediate luminosity values, the atmospheres can be decomposed in 3 layers: an optically thin layer at the outer edge, a convective layer beneath it and a radiative layer at the bottom. When the luminosity is increased, the convective layer extends inward and outward, as shown in Fig. 1

With increasing luminosity, the temperature at the base of the atmosphere increases, in contrast to the mass of the atmosphere, which decreases. Thus, the basal pressure also decreases with the luminosity (the more massive the atmosphere is, the higher the basal pressure is). We find that the properties of fully convective atmospheres are independent of luminosity, as shown in Figs. 2 and 3, although the vigor of convection depends on L .

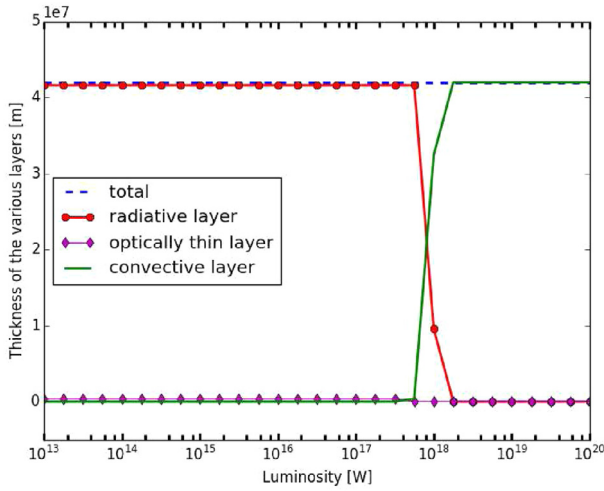


Fig. 1. Thickness of the different layers of the atmosphere (in m) as a function of L (in W). Calculations were carried out for $0.1 M_{\text{Earth}}$ ($6 \cdot 10^{23}$ kg) at a distance of 1 AU and with no depletion ($f=1$).

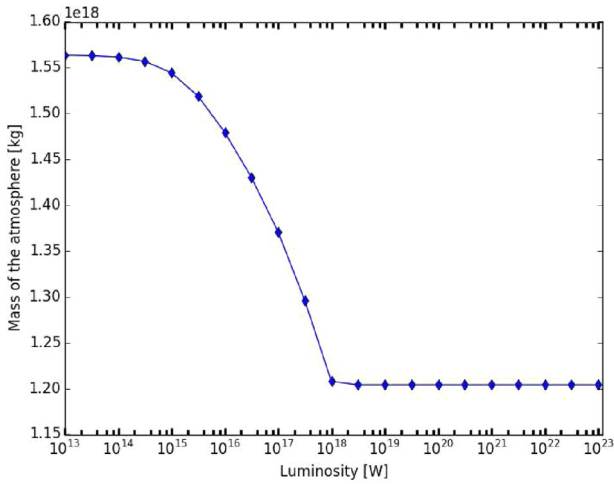


Fig. 2. Mass of the atmosphere (in kg) as a function of L (in W). Calculations were carried out for $0.1 M_{\text{Earth}}$ ($6 \cdot 10^{23}$ kg) at a distance of 1 AU and with no depletion ($f=1$).

For a given luminosity, the temperature at the bottom of atmosphere increases as the protoplanet gets closer to the sun. This is due to a change of boundary conditions at the upper edge of the atmosphere, the nebula getting warmer as the protoplanet gets closer to the sun.

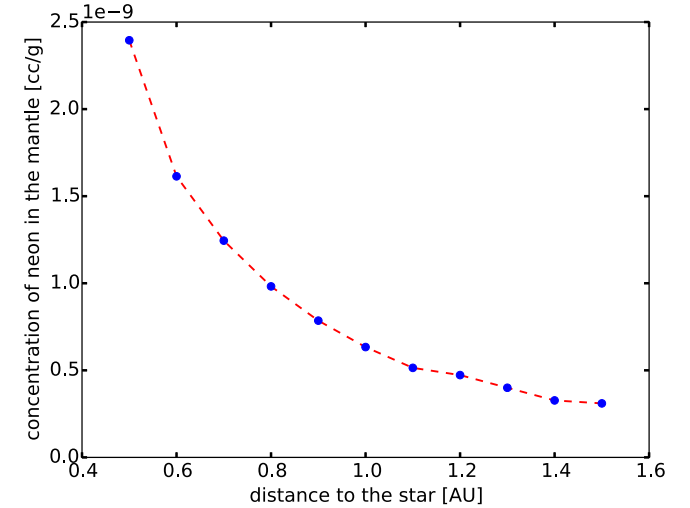
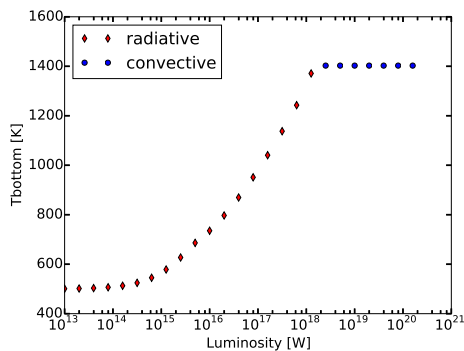


Fig. 4. Concentrations of Neon dissolved in the mantle (in cc/g) as a function of the distance to the star (in AU). These simulations were carried out for a $0.2 M_{\text{Earth}}$ embryo. The average concentration over the distance to the star is $\approx 9 \cdot 10^{-10}$ cc/g.

In summary, we have found two different behaviors. Small embryos (up to roughly $0.1 M_{\text{Earth}}$) cannot capture atmospheres with both a radiative layer at the bottom and a basal temperature higher than 1500 K (see Fig. 3), in contrast to bigger embryos ($0.2 M_{\text{Earth}}$), which can (see Fig. 3). A molten embryo is required for the dissolution of solar gases in significant quantities, and also for mixing the shallow gas-saturated layer with the interior.

3.2. Embryos with $0.2 M_{\text{Earth}}$ masses

Embryos with $0.2 M_{\text{Earth}}$ can have an atmosphere with both a radiative layer at the bottom and a basal temperature higher than 1500 K (see Fig. 3). The lower the luminosity is the more massive the atmosphere is (see Fig. 2). Thus, in order to derive an upper bound for the concentration, we search for the lowest luminosity that leads to a basal temperature of 1500 K. By doing so, we obtain an atmosphere with the largest basal pressure possible above molten ground. From Henry's law, this leads in turn to the highest concentration of gas that can be dissolved in the planet. Fig. 4 shows these concentrations.

We obtain a bulk average Neon concentration of $8.8 \cdot 10^{-10}$ cc/g for $0.2 M_{\text{Earth}}$ embryos. In the following, we shall refer to the ^{22}Ne concentration, which accounts for only 6.7% of the total Neon, and which is therefore $\approx 5.9 \cdot 10^{-11}$ cc/g.

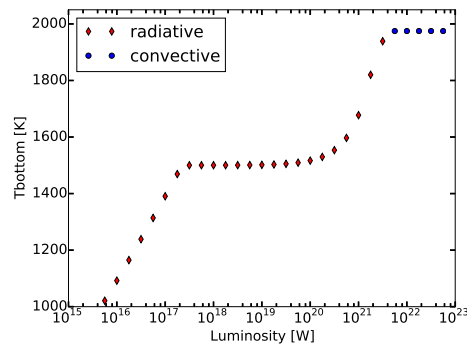


Fig. 3. Basal temperature of the atmosphere (in K) as a function of L (in W). Simulations were carried out at 1 AU and with no depletion ($f=1$). The embryo have a mass of $0.1 M_{\text{Earth}}$ ($6 \cdot 10^{23}$ kg) on the left and $0.2 M_{\text{Earth}}$ on the right. The graphics also show whether the bottom of the atmosphere is radiative or convective.

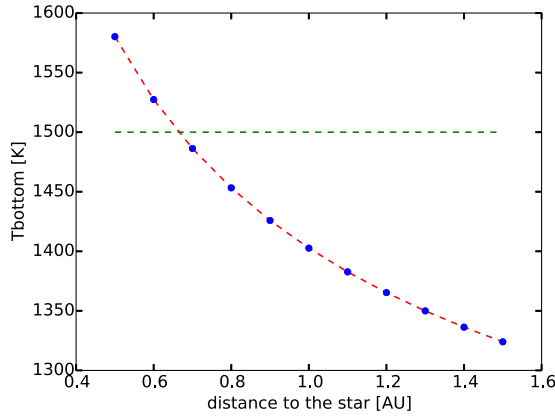


Fig. 5. Basal temperature of the atmosphere (in K) as a function of the distance to the star (in AU). Simulations were carried out for $0.1 M_{\text{Earth}}$ (6×10^{23} kg) and with no depletion ($f=1$). The graph also shows whether the bottom of the atmosphere is radiative or convective.

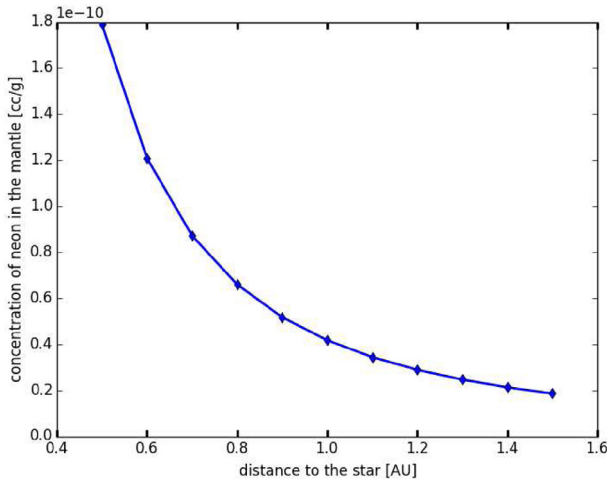


Fig. 6. Concentrations of Neon dissolved in the mantle (in cc/g) as a function of distance to the star (in AU). These simulations were carried out for $0.1 M_{\text{Earth}}$ embryos. The averaged concentration over the distance to the star is $\approx 6 \times 10^{-11}$ cc/g.

3.3. Convective atmospheres in $0.1 M_{\text{Earth}}$ embryos

Mars-sized embryos between 0.7 and 1.5 AU cannot have an atmosphere with both a radiative layer at the bottom and a basal temperature higher than 1500 K (see Fig. 5). Therefore if their ground is molten, their atmosphere can only be fully convective (see the discussion at the end of Section 2.3). Thus, we calculate concentrations using adiabatic profiles for $0.1 M_{\text{Earth}}$ objects between 0.7 and 1.5 AU.

Mars-sized embryos at 0.5 and 0.6 AU can have an atmosphere with both a radiative layer at the bottom and a basal temperature higher than 1500 K. Therefore we use the same method as before to calculate dissolved gas concentrations. However, whereas the radiative layer was of significant thickness for $0.2 M_{\text{Earth}}$ embryos, here, for $0.1 M_{\text{Earth}}$ ones, the atmospheric radiative layer with a basal temperature of 1500 K is thin compared to the convective one. Hence the concentrations found are close to those which would be calculated with adiabatic temperature profiles. We are in a range of luminosity values where the atmospheric properties do not vary much (we are near the conditions of a fully convective atmosphere, see Fig. 2). Fig. 6 shows Neon concentrations as a function of the distance to the star for such bodies.

Our calculations show that $0.1 M_{\text{Earth}}$ embryos can dissolve an average Neon concentration of $\approx 6 \times 10^{-11}$ cc/g, a value that will

now be discussed. This content corresponds to the bulk Neon concentration, whereas we shall refer to measured values of the ^{22}Ne concentration. ^{22}Ne accounts for only 6.7% of the total Neon and its average dissolved concentration is $\approx 4 \times 10^{-12}$ cc/g.

3.4. Neon content of the Earth's primitive mantle

The Neon concentration in primitive mantle can be estimated in two different ways. A first method consists of a simple Neon budget and relies on the assumption that all the atmospheric Neon was degassed from the mantle. The $^{20}\text{Ne}/^{22}\text{Ne}$ ratio of the atmosphere is different from the mantle value, which can be attributed to either a later veneer of chondritic Neon (Marty, 2012) or to the loss of Neon from the atmosphere (Hunten et al., 1987). The amount of solar Neon that has been degassed from the mantle can be estimated in both cases.

In the case of a late veneer, with no subsequent Neon loss, a simple mixing equation can be written to describe the composition of atmospheric Neon:

$$R_{\text{atmosphere}} = \alpha R_{\text{solar}} + (1 - \alpha) RA = 9.8, \quad (13)$$

where RA is the "chondritic" neon isotopic composition, R_{solar} is the solar isotopic composition and α is the proportion of ^{22}Ne coming from solar Neon. Using $RA = 8.5$ (Neon-A, see Black, 1972) and $R_{\text{solar}} \sim 13.8$, we obtain $\alpha = 0.25$. This implies that the amount of primordial (solar) ^{22}Ne degassed from the mantle is 0.25 times the atmospheric ^{22}Ne budget, which gives $0.25 \times 6.65 \times 10^{18}$ ccSTP. Assuming that all the mantle has been thoroughly degassed and taking the mantle mass to be $= 4 \times 10^{24}$ kg, this gives a solar-derived ^{22}Ne concentration of 4×10^{-10} ccSTP/g in the primitive mantle. If only the upper mantle has been degassed ($M = 10^{24}$ kg), the concentration of primitive ^{22}Ne concentration is 1.6×10^{-9} ccSTP/g.

If some Neon has been lost from the atmosphere, one can estimate the fraction of atmospheric Neon that remains using a simple Rayleigh distillation process. This allows one to correct the present day amount of atmospheric ^{22}Ne for Neon loss. We can write:

$$R_{\text{atmosphere}} = R_{\text{solar}} \times f^{\beta-1} \quad (14)$$

where β is the fractionation factor, which will be taken to equal to $\sqrt{22/20}$ (Sarda et al., 1988), and $f = ^{22}\text{Ne}/^{22}\text{Ne}_0$ is the remaining Neon fraction. Using the same isotopic ratios as above, we obtain $f = 0.001$ indicating of massive Neon loss from the atmosphere. In this case, the primitive Neon content of the atmosphere was 6.65×10^{21} ccSTP and the concentration of primitive ^{22}Ne is 1.6×10^{-6} ccSTP/g. In a more complex model, we specify the mechanism of Neon loss. Assuming that Neon loss is due to hydrodynamic escape, one finds that the fraction of initial Neon that remains in the Earth's mantle today is ~ 0.02 (Hunten et al., 1987), corresponding to a ^{22}Ne content of $\sim 8 \times 10^{-8}$ ccSTP/g in the primitive mantle.

The amount of primitive Neon can be calculated with a completely different method. The present-day ^{22}Ne concentration in the mantle source of mid-ocean ridge basalts is estimated to be 10^{-11} ccSTP/g (Moreira and Kurz, 2013). If 99% of the mantle has been degassed, the primitive ^{22}Ne content is 10^{-9} ccSTP/g, in better agreement with the first calculation above. And a mantle degassed at 99.9% suggests a primitive ^{22}Ne concentration of 10^{-8} ccSTP/g.

Depending of the process that accounts for the present-day atmospheric Neon isotopic ratio, be it a loss or gain of Neon, estimates for the ^{22}Ne content of the primitive mantle vary between $\sim 4 \times 10^{-10}$ and $\sim 10^{-7}$ ccSTP/g. These values can be compared to the mean concentrations of 4×10^{-12} ccSTP/g and 6×10^{-11} ccSTP/g due to dissolution of solar gases in embryos with masses of $0.1 M_{\text{Earth}}$ and $0.2 M_{\text{Earth}}$, respectively.

3.5. Discussion

Our goal was to determine whether the process of atmospheric dissolution was sufficiently efficient to produce concentration of dissolved Neon matching current estimations. To do so we used Henry's law (6) and assumed that the whole mantle was equilibrated. This gave us an upper bound for the concentration of Neon that can be dissolved in that process. Indeed, even though fluid motion inside the magma ocean can be turbulent with a short overturn time, equilibration is not assured. The ocean may crystallize or be partly stably stratified before every fluid parcel has the time to experience being in the boundary layer where the exchange of Neon with the atmosphere occurs (see for example the models of Nakajima and Stevenson, 2015).

Furthermore, we did not consider the influence of impacts. Large impacts can be good at introducing volatiles into the planet. The main idea behind this mechanism is the following. As an impactor hits the protoplanet, it pulverises the mantle and generated molten droplets. As these pyroclasts fall back in what we can call the sedimentation phase, they can trap some atmospheric gas in the space left between neighbouring droplets. This available space is initially determined by packing constraints. In a layer that forms in this way, compaction reduces the amount of space available to gas, so that a smaller amount of gas is effectively trapped. How much Neon and how much atmosphere can be introduced forcefully into the planet is an interesting problem involving many subtleties. A simple calculation allows useful estimates of the importance of such a mechanism.

Let us take our protoplanet to be of $0.1 M_{\text{Earth}}$ and let us take a rather massive impactor of $0.01 M_{\text{Earth}}$. Let us further assume that the volume of magma pulverised during the impact is equal to ten times the volume of the impactor (the exact factor depends on a host of variables, as shown by Melosh, 1989). Note that this would mean, in that case, that you pulverised the whole protoplanet, giving a maximum for the amount of gas you can capture in that process. The random packing of identical spheres leads to 36% of captured gas by volume. For a more efficient packing process, this fraction can be as low as 25% of interstitial space (the Kepler limit). It is highly likely, however, that the pyroclasts are polydispersed with a large range of sizes, which allows for much more efficient packing. One can easily achieve packing of 90% or more (see de Laet et al., 2014). With molten droplets, some amount of compaction must occur and this will reduce the amount of captured gas. The process can easily go to completion with virtually no gas left, as shown by welded lava flows that are fed by lava fountains. In the following, we take 10% of captured gas as a starting estimate. For a volume of pulverized mantle equal to 10 times the volume of the impactor, the end result is a captured gas volume equal to the volume of the impactor.

Then using the ideal gas law and using the relative Neon abundance in a solar like nebula ($x \simeq 10^{-4}$) we can determine a concentration of Neon trapped during the accumulation phase: $C_{\text{Neon}} = 10^{-11}$ ccSTP/g. We expect that compaction can be much more effective than allowed here, which would decrease the estimate of captured Neon. This estimate is much lower than the one given by Henry's law ($6 \cdot 10^{-11}$ ccSTP/g). The trapping mechanism certainly helps to reach the equilibrium described by Henry's law and is certainly of importance in the process of dissolving the atmosphere into the mantle. However it cannot give a higher concentration than the one given by Henry's law.

Thus, the concentration we calculated equilibrating the whole mantle gave us higher bounds for the concentration of dissolved Neon resulting of the atmospheric dissolution process.

We have studied embryos of 0.1 and $0.2 M_{\text{Earth}}$ and saw that they cannot provide enough Neon to account for the Neon content of the Earth's mantle. Larger embryos, because of their

bigger mass, could capture a more massive atmosphere and thus give higher concentrations. However, standard cases of recent models of planetary formation only produce Earth embryos as small as 0.1 to 0.2 Earth mass for the biggest objects when the gaseous disk is still massive and present (e.g. Walsh and Levison, 2016). Eventhough we cannot rule out the existance of bigger embryos while the gaseous disk is still present, such embryos appears to be rare in the simulations. The standard value for the mass of the biggest embryo that emerges in the simulation is of 0.1 , 0.2 or even $0.3 M_{\text{Earth}}$ before the gaseous disk disappears (assuming a disappearance time scale of about 3 Myrs). We thus studied a standard embryo of 0.1 to $0.2 M_{\text{Earth}}$.

4. Conclusion

We have evaluated whether the dissolution of solar gases captured from the accretion disk into molten planetary embryos can account for the amount of solar-like Neon that is found today in the Earth's mantle. Model calculations indicate that two different situations arise depending on the embryo mass. Large embryos ($M \geq 0.1 M_{\text{Earth}}$) can have both a molten surface and a static radiative atmosphere, in opposition to small embryos ($M \lesssim 0.1 M_{\text{Earth}}$). In the latter case, and assuming that the embryo surface is molten due to accretion, the atmosphere must undergo vigorous convection and its properties are independent of luminosity. An upper bound for the concentration of dissolved Neon is obtained by assuming a fully molten embryo that equilibrates with its proto-atmosphere. This upper bound increases with increasing embryo mass. It is less than 1% and about 10% of the Ne concentration of the Earth's primitive (undegassed) mantle for $0.1 M_{\text{Earth}}$ and $0.2 M_{\text{Earth}}$ embryos, respectively. At distances between 0.5 and 1.5 AU from the Sun, where the Earth was formed, embryos with $0.2 M_{\text{Earth}}$ are not expected to appear before gas is lost from the accretionary disk save for exceptional circumstances (Weidenschilling et al., 1997; Walsh and Levison, 2016). The Earth was therefore dominantly made out of smaller embryos, implying very small concentrations of dissolved Neon. Considering for the sake of example that the Earth was made of one $0.2 M_{\text{Earth}}$ embryo and eight $0.1 M_{\text{Earth}}$ ones, the Neon concentration of the Earth's primitive mantle would only be about 10^{-11} cc/g, which is less than 2.5% of our best current estimates for the Earth's primitive mantle. Considering this, it is clear that thermodynamic equilibrium with the captured atmospheres of standard planetary embryos cannot account for the Neon contents of the Earth's mantle. For this mechanism to work efficiently enough to reproduce what we observe, one needs a planetary formation model with a faster growing rate for the embryos. Thus, one must instead appeal to solar wind irradiation of parent body precursors (either on regoliths or on dust before the formation of planetesimals). This process is able to incorporate large amounts of solar Neon, as demonstrated by Moreira and Charnoz (2016).

Acknowledgments

E. J. is grateful to IGP for their welcome in their facilities during the summer this work was made. E.J. thanks ENSL for providing the opportunity of this visit and would like to thank both institutes for their support. Financial support from LabEx UnivEarthS is gratefully acknowledged. The authors thank the reviews for their fruitful and interesting remarks.

References

- Amelin, Y., Krot, A.N., Hutcheon, I.D., Ulyanov, A.A., 2002. Lead isotopic ages of Chondrules and Calcium-Aluminum-rich inclusions. *Science* 297, 1678–1683. doi:10.1126/science.1073950.

- Baillié, K., Charnoz, S., Pantin, E., 2015. Time evolution of snow regions and planet traps in an evolving protoplanetary disk. *Astron. Astrophys.* 577, A65. doi:10.1051/0004-6361/201424987. arXiv: 1503.03352.
- Black, D.C., 1972. On the origins of trapped Helium, Neon and Argon isotopic variations in meteorites - II. Carbonaceous meteorites. *Geochim. Cosmochim. Acta* 36, 377–394. doi:10.1016/0016-7037(72)90029-4.
- Brauer, F., Dullemond, C.P., Henning, T., 2008. Coagulation, fragmentation and radial motion of solid particles in protoplanetary disks. *Astron. Astrophys.* 480, 859–877. doi:10.1051/0004-6361:20077759. arXiv: 0711.2192.
- Charnoz, S., Tassilif, E., 2011. Dead zones in protoplanetary disks: accumulation and coagulation of dust. In: *EPSC-DPS Joint Meeting 2011*, p. 117.
- Clarke, W.B., Beg, M.A., Craig, H., 1969. Excess ^3He in the sea: evidence for terrestrial primordial helium. *Earth Planet. Sci. Lett.* 6, 213–220. doi:10.1016/0012-821X(69)90093-4.
- Colin, A., Moreira, M., Gautheron, C., Burnard, P., 2015. Constraints on the noble gas composition of the deep mantle by bubble-by-bubble analysis of a volcanic glass sample from Iceland. *Chem. Geol.* 417, 173–183.
- Craig, H., Clarke, W.B., Beg, M.A., 1975. Excess ^3He in deep water on the East Pacific rise. *Earth Planet. Sci. Lett.* 26, 125–132. doi:10.1016/0012-821X(75)90079-5.
- Gorti, U., Dullemond, C.P., Hollenbach, D., 2009. Time evolution of viscous circumstellar disks due to photoevaporation by far-ultraviolet, extreme-ultraviolet, and X-ray radiation from the central star. *Astrophys. J.* 705, 1237–1251. doi:10.1088/0004-637X/705/2/1237. arXiv: 0909.1836.
- Greenberg, R., Weidenschilling, S.J., Chapman, C.R., Davis, D.R., 1984. From icy planetesimals to outer planets and comets. *Icarus* 59, 87–113. doi:10.1016/0019-1035(84)90058-7.
- Hayashi, C., 1981. Structure of the Solar Nebula, growth and decay of magnetic fields and effects of magnetic and turbulent viscosities on the nebula. *Progress Theor. Phys. Suppl.* 70, 35–53. doi:10.1143/PTPS.70.35.
- Hayashi, C., Nakazawa, K., Mizuno, H., 1979. Earth's melting due to the blanketing effect of the primordial dense atmosphere. *Earth Planet. Sci. Lett.* 43, 22–28. doi:10.1016/0012-821X(79)90152-3.
- Hillenbrand, L. A., 2005. Observational constraints on dust disk lifetimes: implications for planet formation. arXiv:astro-ph/0511083, Astrophysics e-prints.
- Honda, M., McDougall, I., Patterson, D.B., Dougeris, A., Clague, D.A., 1991. A solar component in the Earth: Neon isotope anomalies in Loihi and Kilauea basalts, Hawaii. In: *Lunar and Planetary Science Conference*, 22.
- Hunten, D.M., Pepin, R.O., Walker, J.C.G., 1987. Mass fractionation in hydrodynamic escape. *Icarus* 69, 532–549. doi:10.1016/0019-1035(87)90022-4.
- Ikoma, M., Genda, H., 2006. Constraints on the mass of a habitable planet with water of Nebular origin. *Astrophys. J.* 648, 696–706. doi:10.1086/505780. astro-ph/0606117.
- Jambon, A., Weber, H., Braun, O., 1986. Solubility of He, Ne, Ar, Kr and Xe in a basalt melt in the range 1250–1600 C - geochemical implications. *Geochim. Cosmochim. Acta* 50, 401–408. doi:10.1016/0016-7037(86)90193-6.
- Johansen, A., Klahr, H., 2011. Planetesimal formation through streaming and gravitational instabilities. *Earth Moon Planets* 108, 39–43. doi:10.1007/s11038-010-9370-3.
- Johansen, A., Oishi, J.S., Mac Low, M.-M., Klahr, H., Henning, T., Youdin, A., 2007. Rapid planetesimal formation in turbulent circumstellar disks. *Nature* 448, 1022–1025. doi:10.1038/nature06086. arXiv: 0708.3890.
- Kleine, T., Touboul, M., Bourdon, B., Nimmo, F., Mezger, K., Palme, H., Jacobsen, S.B., Yin, Q.-Z., Halliday, A.N., 2009. Hf-W chronology of the accretion and early evolution of asteroids and terrestrial planets. *Geochim. Cosmochim. Acta* 73, 5150–5188. doi:10.1016/j.gca.2008.11.047.
- Kurz, M.D., Curtice, J., Fornari, D., Geist, D., Moreira, M., 2009. Primitive Neon from the center of the Galápagos hotspot. *Earth Planet. Sci. Lett.* 286, 23–34. doi:10.1016/j.epsl.2009.06.008.
- de Laat, D., de Oliveira Filho, F.M., Vallentin, F., 2014. Upper bounds for packings of spheres of several radii. In: *Forum of Mathematics, Sigma*, 2. Cambridge University Press, p. e23.
- Levison, H.F., Kretke, K.A., Walsh, K.J., Bottke, W.F., 2015. Growing the terrestrial planets from the gradual accumulation of sub-meter sized objects. *Proc. Nat. Acad. Sci.* 112, 14180–14185. doi:10.1073/pnas.1513364112. arXiv: 1510.02095.
- Lissauer, J.J., 1987. Timescales for planetary accretion and the structure of the protoplanetary disk. *Icarus* 69, 249–265. doi:10.1016/0019-1035(87)90104-7.
- Marty, B., 2012. The origins and concentrations of water, carbon, nitrogen and noble gases on Earth. *Earth Planet. Sci. Lett.* 313, 56–66. doi:10.1016/j.epsl.2011.10.040. arXiv: 1405.6336.
- Melosh, H.J., 1989. *Impact cratering: a geologic process*. Oxford Monographs on Geology and Geophysics 11.
- Morbidelli, A., Bottke, W.F., Nesvorný, D., Levison, H.F., 2009. Asteroids were born big. *Icarus* 204, 558–573. doi:10.1016/j.icarus.2009.07.011. arXiv: 0907.2512.
- Moreira, M., Charnoz, S., 2016. The origin of the Neon isotopes in chondrites and on Earth. *Earth Planet. Sci. Lett.* 433, 249–256. doi:10.1016/j.epsl.2015.11.002.
- Moreira, M.A., Kurz, M.D., 2013. *Noble Gases as Geochemical Tracers*. Springer.
- Mukhopadhyay, S., 2012. Early differentiation and volatile accretion recorded in deep-mantle Neon and Xenon. *Nature* 486 (7401), 101–104.
- Nakajima, M., Stevenson, D.J., 2015. Melting and mixing states of the Earth's mantle after the moon-forming impact. *Earth Planet. Sci. Lett.* 427, 286–295.
- Raquin, A., Moreira, M., 2009. Atmospheric $^{38}\text{Ar}/^{36}\text{Ar}$ in the mantle: implications for the nature of the terrestrial parent bodies. *Earth Planet. Sci. Lett.* 287, 551–558. doi:10.1016/j.epsl.2009.09.003.
- Sarda, P., Staudache, T., Allègre, C.J., 1988. Neon isotopes in submarine basalts. *Earth Planet. Sci. Lett.* 91, 73–88. doi:10.1016/0012-821X(88)90152-5.
- Sasaki, S., 1999. Presence of a primary solar-type atmosphere around the earth: evidence of dissolved noble gas. *Planet. Space Sci.* 47, 1423–1431. doi:10.1016/S0032-0633(99)00084-7.
- Sasaki, S., Nakazawa, K., 1990. Did a primary solar-type atmosphere exist around the proto-earth? *Icarus* 85 (1), 21–42.
- Saumon, D., Chabrier, G., van Horn, H.M., 1995. An equation of state for low-mass stars and giant planets. *Astrophys. J. S* 99, 713. doi:10.1086/192204.
- Trieloff, M., 2000. Evidence for Ne-B in Earth's interior: constraints on the timing of accretion and volatile loss in the early solar system? *Meteoritics Planet. Sci. Suppl.* 35, A159.
- Walsh, K.J., Levison, H.F., 2016. Terrestrial planet formation from an annulus. *Astron. J.* 152 (3), 68.
- Walsh, K.J., Morbidelli, A., Raymond, S.N., O'Brien, D.P., Mandell, A.M., 2011. The asteroid belt and Mars' small mass explained by large-scale gas-driven migration of Jupiter. In: *Lunar and Planetary Science Conference*. In: *Lunar and Planetary Science Conference*, 42, p. 2585.
- Weidenschilling, S.J., 1977. The distribution of mass in the planetary system and solar Nebula. *Astrophys. Space Sci.* 51, 153–158. doi:10.1007/BF00642464.
- Weidenschilling, S.J., Spaute, D., Davis, D.R., Marzari, F., Ohtsuki, K., 1997. Accretional evolution of a planetesimal swarm. *Icarus* 128, 429–455. doi:10.1006/icar.1997.5747.
- Yokochi, R., Marty, B., 2004. A determination of the Neon isotopic composition of the deep mantle. *Earth Planet. Sci. Lett.* 225, 77–88. doi:10.1016/j.epsl.2004.06.010.